

Ph. Mertens, G. Arnoux, S. Brezinsek, M. Clever, J.W. Coenen, S. Devaux,  
T. Eich, M. Groth, A. Huber, S. Jachmich, M. Lehnen, P.J. Lomas,  
G. Maddaluno, H. Maier, S. Marsen, G.F. Matthews, R. Neu, V. Riccardo,  
G. van Rooij, C. Ruset, B. Sieglin and JET EFDA contributors

# Power Handling of the Tungsten Divertor in JET



# Power Handling of the Tungsten Divertor in JET

Ph. Mertens<sup>1</sup>, G. Arnoux<sup>2</sup>, S. Brezinsek<sup>1</sup>, M. Clever<sup>1,2</sup>, J.W. Coenen<sup>1</sup>, S. Devaux<sup>3</sup>,  
T. Eich<sup>3</sup>, M. Groth<sup>4</sup>, A. Huber<sup>1</sup>, S. Jachmich<sup>5</sup>, M. Lehnen<sup>1</sup>, P.J. Lomas<sup>2</sup>,  
G. Maddaluno<sup>6</sup>, H. Maier<sup>3</sup>, S. Marsen<sup>3</sup>, G.F. Matthews<sup>2</sup>, R. Neu<sup>3</sup>, V. Riccardo<sup>2</sup>,  
G. van Rooij<sup>7</sup>, C. Ruset<sup>8</sup>, B. Sieglin<sup>3</sup> and JET EFDA contributors\*

***JET-EFDA, Culham Science Centre, OX14 3DB, Abingdon, UK***

<sup>1</sup>*Institute for Energy and Climate Research IEK-4 (Plasma Physics), Association EURATOMFZJ,  
D-52425 Jülich, Germany*

<sup>2</sup>*EURATOM-CCFE Fusion Association, Culham Science Centre, OX14 3DB, Abingdon, OXON, UK*

<sup>3</sup>*Max-Planck-Institut für Plasmaphysik, EURATOM Association, D-85748 Garching, Germany*

<sup>4</sup>*Aalto University, Association EURATOM-Tekes, PO Box 14100, FIN-00076 Aalto, Finland*

<sup>5</sup>*LPP-ERM/KMS, Association EURATOM-Belgian State, B-1000 Brussels, Belgium*

<sup>6</sup>*Association EURATOM-ENEA sulla Fusione, C.R. Frascati (Roma), I-00044 Frascati, Italy*

<sup>7</sup>*FOM Institute DIFFER, EURATOM Association, NL-3430 BE Nieuwegijn, The Netherlands*

<sup>8</sup>*Institute for Laser, Plasma and Radiation Physics, EURATOM-MEdC Association, Bucharest*

*\* See annex of F. Romanelli et al, "Overview of JET Results",  
(24th IAEA Fusion Energy Conference, San Diego, USA (2012)).*

Preprint of Paper to be submitted for publication in Proceedings of the  
24th IAEA Fusion Energy Conference (FEC2012), San Diego, USA

8th October 2012 - 13th October 2012

“This document is intended for publication in the open literature. It is made available on the understanding that it may not be further circulated and extracts or references may not be published prior to publication of the original when applicable, or without the consent of the Publications Officer, EFDA, Culham Science Centre, Abingdon, Oxon, OX14 3DB, UK.”

“Enquiries about Copyright and reproduction should be addressed to the Publications Officer, EFDA, Culham Science Centre, Abingdon, Oxon, OX14 3DB, UK.”

The contents of this preprint and all other JET EFDA Preprints and Conference Papers are available to view online free at [www.iop.org/Jet](http://www.iop.org/Jet). This site has full search facilities and e-mail alert options. The diagrams contained within the PDFs on this site are hyperlinked from the year 1996 onwards.

## **ABSTRACT.**

With incident power densities of 5–10 MW/m<sup>2</sup> or higher, divertor target plates of large tokamaks are driven close to the material limits. The power handling performance is essential to their characterisation. The thermal performance of tungsten is critical to the decision as to whether to start ITER with an all tungsten divertor. In the new ITER-like Wall in JET, the divertor tiles consist of carbon-fibre composites coated with tungsten except for a specific row within the range of the outer strike point (horizontal target) where bulk tungsten is used.

The multilayer coating (Mo/W) is 12–25 μm thick depending on the poloidal position. Ion beam tests have shown that the risk of delamination is low (<1% area) as long as the coating is maintained below 1200°C and carbidisation is negligible. The tiles are coated by combined magnetron sputtering and ion implantation (CMSII).

The bulk tungsten row consists of 48 tile assemblies. Each one is made of two sets of four stacks of 24 lamellae. The stacks are aligned with the toroidal direction. To minimise the risk of fracture, the brittle tungsten is subjected by the clamping to compression forces only. The surface temperature was initially limited to 1200°C to avoid appreciable grain growth and possible thermo-mechanical fatigue (no higher temperature was recorded, by the infrared systems up to now:  $T_{\text{surf}} < 1200^\circ\text{C}$ ). Densities of deposited energy in the order of 20–30 MJ/m<sup>2</sup> were reached so far. The modelled temperature rise of the plasma-facing tungsten components shows a fair agreement with the records of thermocouples and of infrared cameras. The experimental behaviour is close to the design values in a wide range of operational parameters.

Special protruding lamellae were designed to expose leading edges with a vertical step  $\geq 0.3$  mm with the aim of deliberate melting. These future investigations are intended to support ITER since melting is the highest risk for a solid tungsten divertor.

## **1. INTRODUCTION**

With an incident power density in the range 5–10 MW/m<sup>2</sup>, or even higher for limited time intervals, divertor target plates of present and future large tokamaks are driven close to the material limits. The power handling performance is thus essential to the characterisation and operation of the divertor. In the full tungsten divertor of the new ITER-like Wall in JET [1], these tiles are not actively cooled. They consist of carbon fibre composites (CFC) coated with tungsten [2] in the inner and outer strike point regions (ISP and OSP respectively) and of bulk tungsten for a specific row within the range of the OSP [3] (Fig.1).

## **2. THE COATED TILES**

The multilayer tungsten coating (Mo/W) is 12 or 25 μm thick, depending on the poloidal position. Former ion beam tests have shown that the risk of delamination is extremely low (<1% area) as long as the coating is maintained below 1200°C and carbidisation effects are negligible [4]. The coating is produced by combined magnetron sputtering and ion implantation (CMSII-discharges in

argon) [5, 6]. The resulting Ar content of the layers (<2% at.) is seen by spectroscopic detection of argon traces in the discharges, which are of no concern. W-radiation events were observed which correspond to particles penetrating the main plasma with equivalent diameters around 100  $\mu\text{m}$ . The number of events has decreased with time, hinting at a conditioning effect. As it was ensured during early operation that the temperature limit is not exceeded, no damage was detected in the first measurement campaigns (C28-C30) that could be seen with the In-Vessel Inspection System (IVIS): regular inspections have not revealed any definitive evidence of delamination, which is consistent with tests [7] in the GLADIS and JUDITH facilities. Nevertheless, hot spots can be seen on the coated tiles which are believed to be debris from other sources but tiny blister-like damages cannot be fully ruled out. On the other hand, no significant increase was noticed in spectroscopic signals from carbon [8] which might originate from the CFC substrate.

### 3. THE BULK TUNGSTEN TILE

The bulk tungsten divertor row consists of 48 tile assemblies. Each assembly is made of two sets (tiles) of four stacks of 24 lamellae (Fig.2). The stacks are aligned with the toroidal direction. To minimise the risk of fracture, the brittle tungsten is subjected by the clamping arrangement to compression forces only [9]. The original limit on the surface temperature of the tungsten tile,  $T_{W,\text{surf}} \leq 1200^\circ\text{C}$ , was set to avoid appreciable grain growth and possible thermomechanical fatigue [10]. The highest temperature observed was  $T_{W,\text{max}} \cong 1150^\circ\text{C}$  at the time of writing. Now, the temperature is limited to  $2200^\circ\text{C}$  (a limit on the power density) under appropriate budget accounting with classes delimited at  $1000^\circ\text{C}$ ,  $1200^\circ\text{C}$  and  $1700^\circ\text{C}$  [11].

### 4. RESULTS

In the overall power balance, the radiative power – both in the main chamber and in the divertor –, the NBI shine through and the sharing between divertor legs were duly considered for a quantitative evaluation of the power handling of the divertor (Fig.3). Deposited energy densities in the order of 20-30 MJ/m<sup>2</sup> were measured so far, taking into account the deposition profiles in poloidal direction, an exponential decay to the scrape-off layer (SOL) and to the private flux region (PFR), according to [12, 13] e.g. – both types of profiles are relevant and applicable.

The power density scaled for 1 MW impinging as in Fig.4 (examples next page) reads:

$$q_{\text{sol,pfr}} = 2.52 (\exp(-37.6 (R-R_{\text{osp}})) \{\text{SOL}\} + \exp(+112.8 (R-R_{\text{osp}})) \{\text{PFR}\}) / \text{m}^2 \quad (1)$$

where either the left or right term in the braces applies, respectively to the SOL or PFR. The major radii  $R$  and  $R_{\text{osp}}$  are given in metres. About 80% of the deposited energy may fall on a single row of stacks, 62mm wide in poloidal direction, if a static strike point is intentionally positioned that way.

The moderate temperature rise of the plasma-facing tungsten at these low exposures ( $130^\circ\text{C}$ - $800^\circ\text{C}$ ) is in fair agreement ( $\pm 60^\circ\text{C}$ ) with the initial thermal model used in the development phase.

This holds true for records of embedded thermocouples (some of which are redundant but others were lost in the course of the campaign), for thermographic measurements by infrared (IR) cameras ([14] and Fig.4 for the present case) and for pyrometers. The IR measurements are sensitively dependent on the assumed emissivity. We took values in the range  $\epsilon_w \sim 0.18-0.6$ , the lower value for low temperatures, higher values for high temperatures and for coatings. The assumed temperature dependence of  $\epsilon_w$  is quite close to the curves used for the estimations for ITER.

For some configurations (among low- $\delta$  ‘V5’ and high- $\delta$  ‘HT3R’), the radiated power had to be corrected to higher values by about 10% to account for the loss channel of chargeexchange neutrals and for the sharing between inner and outer divertor legs which is close to the originally assumed 1:2 ratio but is occasionally slightly more symmetric. The absence of correction in  $P_{\text{rad}}$  for all cases tends indeed to move the sharing to more equal loads in the legs but the correction is within the error bars and thus not significant at the powers reached for the moment. The highest permitted loads in terms of deposited energy density  $E_{\text{dep}} \leq 54 \text{MJ/m}^2$  on the bulk tile are determined in the first place by the carrier structure. On account of the segmentation of the tiles, sweeping over two stacks is effective for spreading out the load down to acceptable levels.

The rows of tiles that are not used for a couple of pulses tend to become covered with dust particulates which display little thermal contact to the tile surface and are exaggeratedly bright. Quite the contrary to would-be leading edges in a row of lamellae, these particulates lighten up only in the presence of the plasma. Note that the installed geometry is quite close to the expectations with deviations of the vertical steps across gaps in the order of  $\Delta z \leq 150 \mu\text{m}$ . Accordingly, no leading edges were detected between solid tungsten tiles or even single lamellae in dedicated experiments down to  $q_{95} \geq 2.45$ . This was demonstrated in magnetic field scans from  $B_T = 2.0 \text{ T}$  down to  $B_T = 1.27 \text{ T}$  which corresponds to an increase of the wetted area on a stack from about  $f_{\text{wet}} = 0.67$  (16/24) to  $f_{\text{wet}} = 0.96$  (23/24). We conclude from the above that the divertor tiles perform closely to the design specifications and no significant damage was detected, neither on the coatings (cf. section 3), nor on the solid row of the tungsten divertor.

## 5. DELIBERATE MELTING IN SUPPORT OF ITER

Special protruding lamellae were designed on purpose to expose leading edges with a vertical step  $\geq 0.3 \text{mm}$ : the aim is deliberate melting of the otherwise little used ‘row A’ (the row of stacks A), on the high field side. These lamellae shall be installed during the current shutdown and the experiments are planned for 2013, in support of ITER. The lamellae in front of the exposed facet are slanted in order to allow an adjustment of the misaligned face seen by the plasma by moving the strike point along the lamellae of stack A in poloidal direction (Fig.5a) – a geometric amplification of the heat flux density of 10–20 is expected. Figure 5b demonstrates that operation on the upper (HFS) stack A is indeed a feasible scenario. The idea is to quantify the movement of melt layers during repeated shallow melt events and the associated net material loss rate, which means that the driving force responsible for the melt layer flow must be identified by discriminating, if possible, between a  $\mathbf{j} \times \mathbf{B}$

force caused by the thermoelectronic emission and a displacement under plasma pressure (Fig.6 and [16]). Shallow melting might be achieved in a two-step process: preheating with steady state heat loads and go past the melting point with the additional heat load of large ELMs. The estimated temperature of the protruding tungsten lamella in such a scenario would reach  $T_{W,surf} \approx 2400^{\circ}\text{C}$  (exposed edge) after 5s exposure to a moderate steady state flux density of  $q_0 = 2\text{MW}/\text{m}^2$  [17] on top of the tiles. A realistic angle of incidence of the field lines for stack A of  $\theta_{\perp} = 1.7^{\circ}$  was assumed for this estimation. In terms of thermal impact factors,  $q_0 \sqrt{t} \sim \Delta T \cdot \sqrt{(\pi k \rho C)}$ , where the symbols bear their usual meaning ( $k$  is the thermal conductivity of tungsten,  $\rho$  the density and  $C$  the heat capacity), it can be shown that the melting point around  $50\text{MWm}^{-2} \text{s}^{1/2}$  can be exceeded with ELMs.

A really critical question for ITER is whether a melt damage evolves in a benign way or whether power handling progressively deteriorates due to the degradation of surface geometry and/or properties. Assuming that melting cannot be avoided at some level, ITER needs to know how serious the consequences are for subsequent operation. Although quite challenging, the dedicated experiment planned in JET may provide in fine a significant contribution to the answer.

## CONCLUSIONS

The thermal performance of tungsten is critical to the decision as to whether to start ITER with an all tungsten divertor. In the new ITER-like Wall in JET, the divertor tiles consist of carbon-fibre composites coated with tungsten except for a specific row within the range of the outer strike point where bulk tungsten is used for the horizontal target. The experimental behaviour of the tungsten divertor of the JET ITER-like Wall is close to the design values in a wide range of operational parameters (notably around a deposited energy density of  $30\text{MJ}/\text{m}^2$  and surface temperatures in excess of  $1100^{\circ}\text{C}$ ). No significant damage could be identified during inspections. The operating limits will be gradually released in the course of the next campaign, especially as far as the bulk tungsten row is concerned. Special protruding lamellae were designed to expose leading edges with a vertical step  $\geq 0.3\text{mm}$  with the aim of deliberate melting. These future investigations are intended to support ITER since melting is the highest risk for a solid tungsten divertor.

## ACKNOWLEDGEMENTS

This work was supported by EURATOM and carried out within the framework of the European Fusion Development Agreement. The views and opinions expressed herein do not necessarily reflect those of the European Commission.

## REFERENCES

- [1]. Matthews, G.F. et al., “JET ITER-like wall—overview and experimental programme”, *Physica Scripta* **T145** (2011) 014001 (6pp)
- [2]. Ruset, C., et al., “Development of W coatings for fusion applications”, *Fusion Engineering and Design* **86** (2011) 16771680



- [3]. Mertens, PH., et al., “A bulk tungsten divertor row for the outer strike point in JET”, *Fusion Engineering and Design* **84** (2009) 128993
- [4]. Maier, H., et al., “Tungsten coatings for the JET ITER-like wall project”, *Journal of Nuclear Materials* **363** (2007) 12461250
- [5]. Ruset, C., et al., “Tungsten coatings deposited on CFC tiles by the combined magnetron sputtering and ion implantation technique”, *Physica Scripta* **T128** (2007) 171174
- [6]. I. Tiseanu, I., et al., “Advanced X-ray imaging of metal-coated/impregnated plasma-facing composite materials”, *Physica Scripta* **T145** (2011) 014073
- [7]. Maier, H., et al., “Qualification of tungsten coatings on plasma-facing components for JET”, *Physica Scripta* **T138** (2009) 014031 (5pp)
- [8]. Coenen, J.W., et al., “Long term Evolution of the Impurity Composition and Transient Impurity Events with the ITER-like Wall at JET”, this conference
- [9]. Mertens, PH., “Clamping of solid tungsten components for the bulk W divertor row in JET – precautionary design for a brittle material”, *Physica Scripta* **T138** (2009) 014032 (5pp)
- [10]. Mertens, PH., et al., “Bulk Tungsten in the JET Divertor : Potential Influence of the Exhaustion of Ductility and Grain Growth on the Lifetime”, *Journal of Nuclear Materials* (submitted)
- [11]. Mertens, PH., et al., “Detailed design of a solid tungsten divertor row for JET in relation to the physics goals”, *Physica Scripta* **T145** (2011) 014002 (7pp)
- [12]. Mertens, PH., et al., “Power handling of a segmented bulk W tile for JET under realistic plasma scenarios”, *Journal of Nuclear Materials* **415** (2011) S943S947
- [13]. Eich, T., et al., “Type-I ELM power deposition profile width and temporal shape in JET”, *Journal of Nuclear Materials* **415** (2011) S856S859
- [14]. Balboa, I., et al., “Upgrade of the infrared camera diagnostics for the JET ITER-like wall divertor”, *Review of Scientific Instruments* **83** (2012) 10D530
- [15]. Mertens, PH., et al., “ Power Handling of the Bulk Tungsten Divertor Row at JET: First measurements and comparison to the GTM model ”, submitted to *Fusion Engineering and Design*
- [16]. Coenen, J.W., et al., “Analysis of tungsten melt-layer motion and splashing under tokamak conditions at TEXTOR”, *Nuclear Fusion* **51** (2011) 083008 (11pp)
- [17]. Thompson, V., private communication

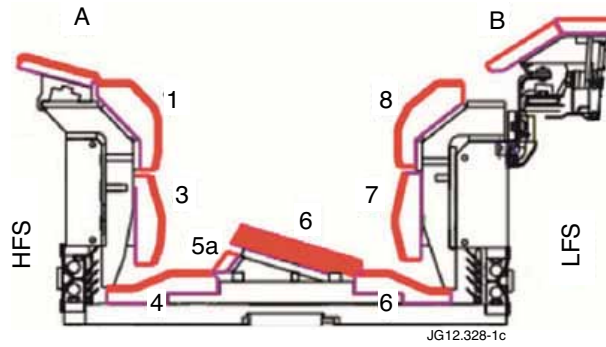


Figure 1: Cross section of the current JET divertor. Tiles 1 and 3, where the inner strike point (ISP) is placed in the following, are coated with Mo/W layers of  $25\mu\text{m}$  and  $12\mu\text{m}$ , respectively. Tile 5 (within the range of the OSP) is made of bulk tungsten. HFS and LFS indicate the high- and low-field sides. Tile by tile: A, 3, 4, 5a, B –  $12\mu\text{m}$  Mo/W; 1, 6, 7, and 8 –  $25\mu\text{m}$  Mo/W or Mo/W/Mo/W; the Mo interlayers are  $\sim 2\mu\text{m}$  thick in all cases.

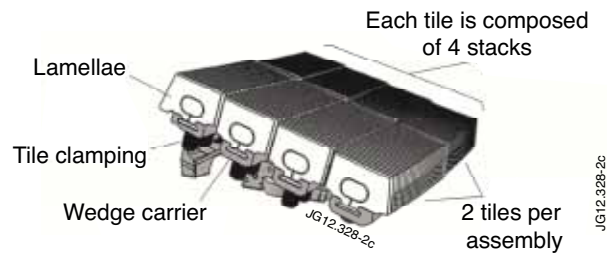


Figure 2: One of the 48 assemblies which compose the solid tungsten row in the divertor (tile 5). The torus axis (high field side) is on the left of the picture.

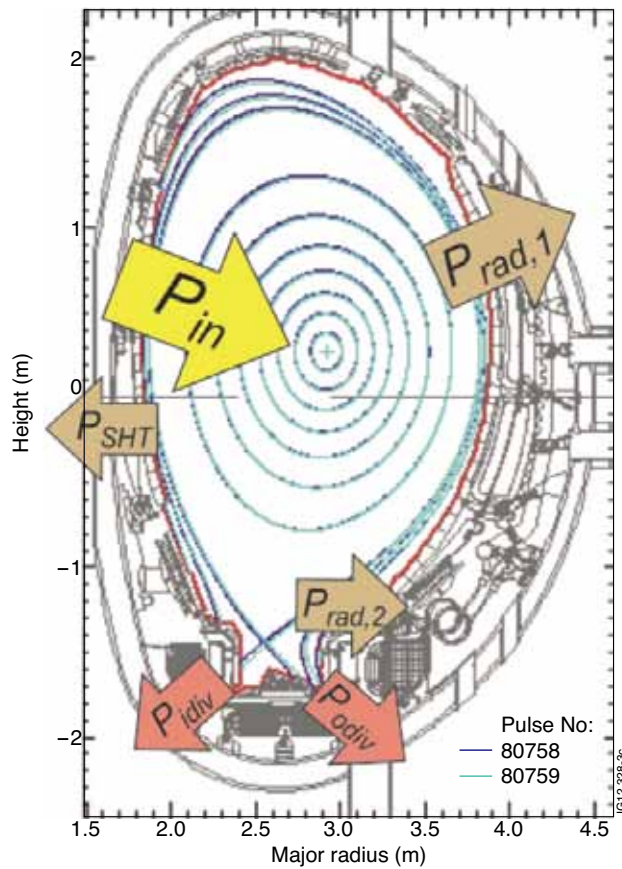


Figure 3: Power fluxes that were considered in the power balance to the outer divertor leg.

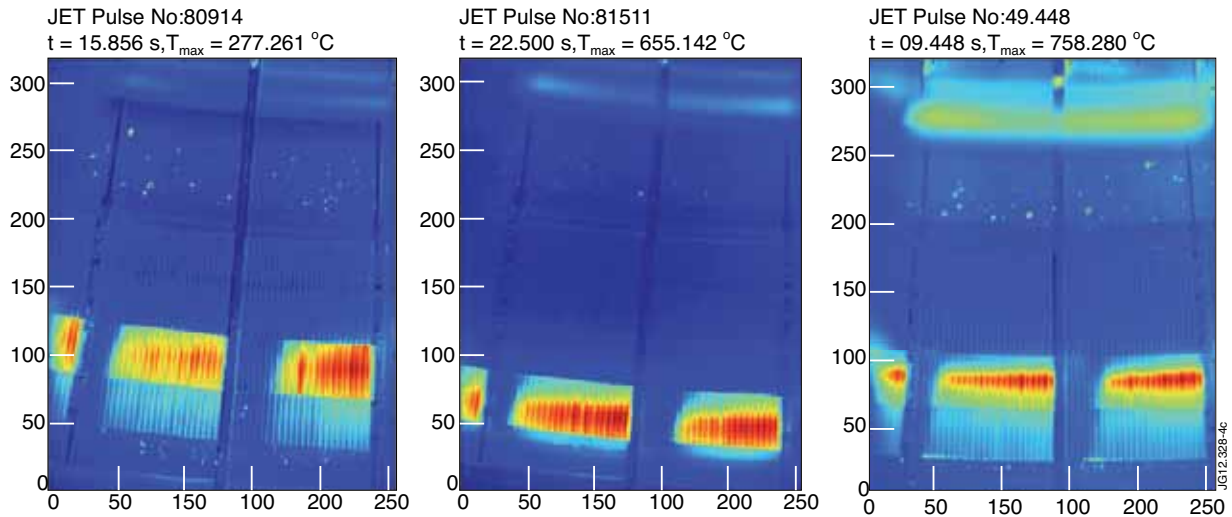


Figure 4: Top views of the bulk tungsten tile under various conditions (different stacks wetted) with an infrared camera (KL9B [14]). Left: sweep over 'stack C'; middle: on 'stack D'; right: static OSP on 'stack C'. The centre of JET is above and the low field side is at the bottom of the pictures.

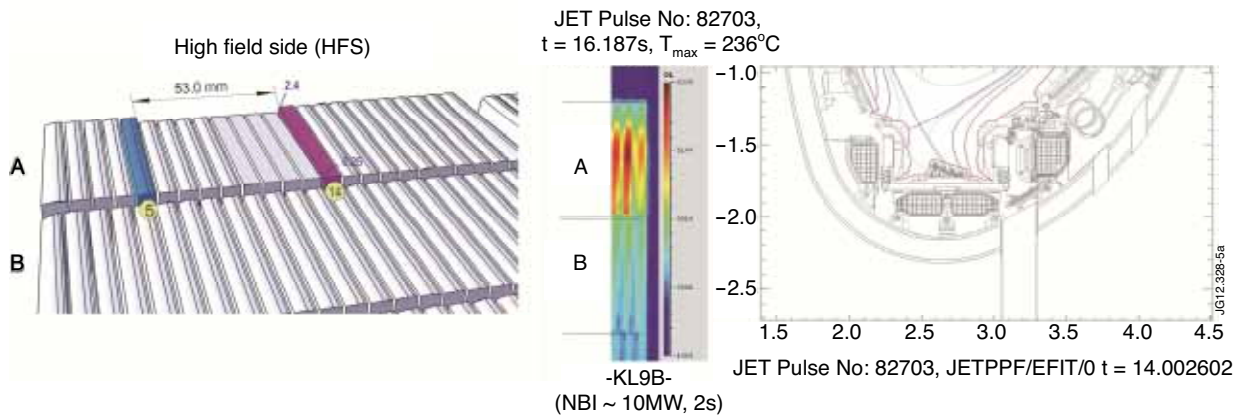


Figure 5: (a) Arrangement of tungsten lamellae for deliberate melting, and (b) operation with OSP moved from stack B (dark solid line) to stack A (light blue) during JET Pulse No: 82703.

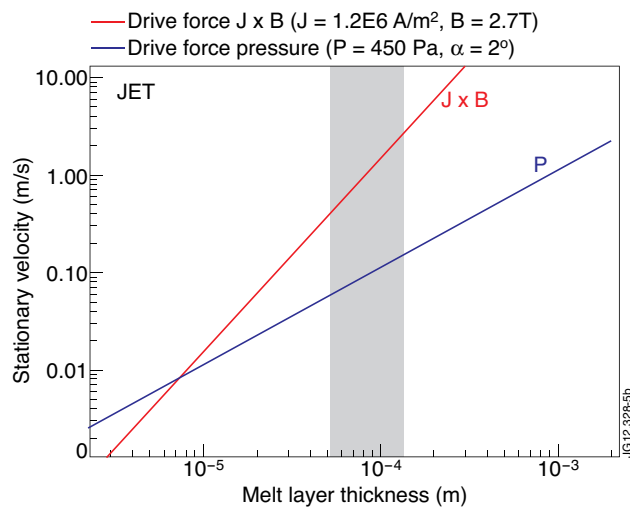


Figure 6: One of the model predictions for the driving force acting on a melt layer in JET. The shaded region indicates the range of expected thickness. (by courtesy of G. Sergienko)